# Bat and pig IFN-induced transmembrane protein 3 restrict cell entry by influenza virus and lyssaviruses

Article (Accepted Version)

JGV Papers in Press. Published January 22, 2015 as doi:10.1099/vir.0.000058

Journal of General Virology

# Bat and pig Interferon-Induced Transmembrane Protein 3 restrict cell entry by influenza virus and lyssaviruses

--Manuscript Draft--

| | |
|---|---|
| **Manuscript Number:** | JGV-D-14-00286R2 |
| **Full Title:** | Bat and pig Interferon-Induced Transmembrane Protein 3 restrict cell entry by influenza virus and lyssaviruses |
| **Short Title:** | Bat and pig IFITM3 restrict zoonotic viruses |
| **Article Type:** | Standard |
| **Section/Category:** | Animal - Negative-strand RNA Viruses |
| **Corresponding Author:** | Camilla Benfield<br>Royal Veterinary College<br>Hatfield, UNITED KINGDOM |
| **First Author:** | Camilla Benfield |
| **Order of Authors:** | Camilla Benfield |
| | Sarah E. Smith |
| | Edward Wright |
| | Rachel S. Wash |
| | Francesca Ferrara |
| | Nigel J. Temperton |
| | Paul Kellam |
| **Abstract:** | Interferon-induced transmembrane protein 3 (IFITM3) is a restriction factor which blocks cytosolic entry of numerous viruses that utilise acidic endosomal entry pathways. In humans and mice, IFITM3 limits influenza-induced morbidity and mortality. Although many IFITM3-sensitive viruses are zoonotic, whether IFITMs function as antiviral restriction factors in mammalian species other than humans and mice is unknown. Here, IFITM3 orthologues in the microbat Myotis myotis and the pig (Sus scrofa domesticus) were identified using rapid amplification of cDNA ends. Amino acid residues known to be important for IFITM3 function were conserved in the pig and bat orthologues. Ectopically-expressed pig and microbat IFITM3 co-localised with transferrin (early endosomes) and CD63 (late endosomes/multivesicular bodies) and trafficked from the plasma membrane into endosomes following live cell staining. Pig and microbat IFITM3 restricted cell entry mediated by multiple influenza HA subtypes and lyssavirus G proteins. Expression of pig or microbat IFITM3 in A549 cells reduced influenza virus yields and nucleoprotein expression. Conversely siRNA knockdown of IFITM3 in pig NPTr cells and primary microbat cells enhanced virus replication, demonstrating that these genes are functional in their species of origin at endogenous levels. In sum, we show that IFITMs function as potent broad-spectrum antiviral effectors in two mammals - pigs and bats - identified as major reservoirs for emerging viruses. |

# Bat and pig Interferon-Induced Transmembrane Protein 3 restrict cell entry by influenza virus and lyssaviruses

Camilla T. O. Benfield[1#], Sarah E. Smith[2], Edward Wright[4], Rachael S. Wash[2], Francesca Ferrara[5], Nigel J. Temperton[5] and Paul Kellam[2,3]

[1]Department of Pathology and Pathogen Biology, The Royal Veterinary College, Hatfield, UK; [2]Wellcome Trust Sanger Institute, Wellcome Trust Genome Campus, Hinxton, Cambridge, UK; [3] MRC/UCL Centre for Medical Molecular Virology, Division of Infection and Immunity, University College London, London, UK; [4] Viral Pseudotype Unit (Fitzrovia), Faculty of Science and Technology, University of Westminster, London, UK; [5] Viral Pseudotype Unit (Medway), School of Pharmacy, University of Kent, Chatham Maritime, Kent, UK

Running Title: Bat and pig IFITM3 restrict zoonotic viruses

# Address correspondence to Camilla Benfield, cbenfield@rvc.ac.uk, Tel: +44 (0)1707 667059, Fax: +44 (0)1707 652090

Contents category: Standard paper

Summary: 198 words

Text: 5500 words

Figures: 8

**Summary**

Interferon-induced transmembrane protein 3 (IFITM3) is a restriction factor which blocks cytosolic entry of numerous viruses that utilise acidic endosomal entry pathways. In humans and mice, IFITM3 limits influenza-induced morbidity and mortality. Although many IFITM3-sensitive viruses are zoonotic, whether IFITMs function as antiviral restriction factors in mammalian species other than humans and mice is unknown. Here, IFITM3 orthologues in the microbat *Myotis myotis* and the pig (*Sus scrofa domesticus*) were identified using rapid amplification of cDNA ends. Amino acid residues known to be important for IFITM3 function were conserved in the pig and bat orthologues. Ectopically-expressed pig and microbat IFITM3 co-localised with transferrin (early endosomes) and CD63 (late endosomes/multivesicular bodies). Pig and microbat IFITM3 restricted cell entry mediated by multiple influenza HA subtypes and lyssavirus G proteins. Expression of pig or microbat IFITM3 in A549 cells reduced influenza virus yields and nucleoprotein expression. Conversely siRNA knockdown of IFITM3 in pig NPTr cells and primary microbat cells enhanced virus replication, demonstrating that these genes are functional in their species of origin at endogenous levels. In sum, we show that IFITMs function as potent broad-spectrum antiviral effectors in two mammals – pigs and bats – identified as major reservoirs for emerging viruses.

## Introduction

Restriction factors are germline-encoded proteins that function in a cell-autonomous manner to suppress virus replication. The interferon-induced transmembrane (IFITM) proteins are a family of small interferon (IFN)-stimulated proteins, which affect diverse cellular processes (reviewed in (Siegrist *et al.*, 2011)) and were recently identified as antiviral restriction factors which inhibit cell entry of multiple pathogenic viruses (Brass *et al.*, 2009).

To date, IFITMs have been reported to restrict the enveloped viruses influenza A, West Nile Virus and Dengue Virus (*Flaviviridae*), SARS-coronavirus, Ebola and Marburg viruses (*Filoviridae*), Vesicular Stomatitis Virus (VSV) and lyssaviruses (*Rhabdoviridae*), HIV-1 and several species of *Bunyaviridae,* as well as a non-enveloped orthoreovirus (*Reoviridae*) (Anafu *et al.*, 2013; Brass *et al.*, 2009; Huang *et al.*, 2011; Jia *et al.*, 2012; Lu *et al.*, 2011; Mudhasani *et al.*, 2013; Smith *et al.*, 2013; Weidner *et al.*, 2010). The common feature of IFITM-sensitive viruses appears to be their dependence on acidic endosomal entry pathways, either for proteolytic cleavage, or pH- or protease-dependent activation of viral entry proteins into their fusogenic form. Accordingly, pseudotyped retroviruses expressing heterologous surface envelope proteins recapitulate the IFITM sensitivity of the authentic virus from which the envelope protein derives, and have been widely used to study IFITM biology (Brass *et al.*, 2009; Feeley *et al.*, 2011; Huang *et al.*, 2011). The IFITMs localise to membranes of late endosomes and lysosomes and prevent the release of viral particles from these compartments into the cytosol (Feeley *et al.*, 2011).

The human *IFITM* gene family comprises *IFITM1, -2, -3, -5,* all of which possess antiviral activity and cluster together on chromosome 11, as well as *IFITM10* whose function remains unknown. Mice possess orthologues of all the human *IFITM* genes and two additional genes, *Ifitm6* and *Ifitm7*. IFITM1-3 are expressed in a wide range of tissues (Bailey *et al.*,

2012; Everitt *et al.*, 2013; Siegrist *et al.*, 2011) whereas IFITM5 expression is limited to osteoblasts (Moffatt *et al.*, 2008). Of all the IFITMs, IFITM3 is the most potent anti-influenza effector *in vitro* (Huang *et al.*, 2011). Ifitm3 has a critical role in limiting influenza-induced morbidity and mortality in mice (Everitt *et al.*, 2012). Since the phenotype of influenza-infected *Ifitm3*$^{-/-}$ mice was indistinguishable from that of mice deleted for the entire locus (comprising *Ifitm1,-2,-3,-5* and *-6*), Ifitm3 apparently dominates influenza resistance *in vivo (Bailey et al., 2012)*. Moreover, the importance of IFITM3 was highlighted by reports showing that an *IFITM3* allele (rs12252-C) is associated with enhanced disease severity caused by pandemic influenza H1N1/09 (Everitt *et al.*, 2012; Zhang *et al.*, 2013b) and highly pathogenic influenza H7N9 (Wang *et al.*, 2014) and is more frequent in Chinese than Caucasian populations.

IFITM proteins comprise a relatively long hydrophilic N-terminal region, two hydrophobic intramembrane domains (IM1 and IM2), separated by a conserved intracellular loop (CIL), and a comparatively short hydrophilic C-terminal region. The IM1 and CIL together constitute the CD225 domain, a functionally poorly-defined domain shared by >300 members of the CD225/pfam04505 protein superfamily. Several alternative topologies have been proposed for the IFITMs (Chen *et al.*, 1984; Li *et al.*, 2013; Takahashi *et al.*, 1990; Yount *et al.*, 2012), but the most recent study suggests that murine Ifitm3 is a type II transmembrane protein, comprising an intracellular N-terminus, an extracellular C-terminus and a membrane-spanning 'IM2' domain (Bailey *et al.*, 2013). IFITM function is regulated by several post-translational modifications. S-palmitoylation of IFITM3 on three membrane proximal cysteine residues enhances membrane affinity and antiviral activity against influenza (Yount *et al.*, 2012; Yount *et al.*, 2010). Conversely, lysine-linked ubiquitination decreases IFITM3's co-localisation with endolysosomes and its antiviral potency (Yount *et al.*, 2012). The Y20 residue, which can be phosphorylated by the tyrosine kinase Fyn, is critical for targeting

IFITM3 to endolysosomes and restriction of endosome-dependent viruses (Jia *et al.*, 2012; John *et al.*, 2013).

Current evidence indicates that IFITMs block viral entry to the cytosol by preventing fusion between viral and host cell membranes. IFITMs multimerise via their IM1 regions (John *et al.*, 2013) and increase membrane rigidity (Li *et al.*, 2013). This suggests a model in which IFITMs either physically resist the deformation of the membrane by the viral fusion machinery or hinder the lateral mobility of viral or cellular proteins within the membrane and thereby block successful pore formation (John *et al.*, 2013; Li *et al.*, 2013; Perreira *et al.*, 2013). Amini-Bavil-Olyaee *et al.* recently reported that IFITM3 interacts with a protein involved with cholesterol homeostasis, vesicle-membrane-protein-associated protein A (VAPA), and thereby causes cholesterol accumulation in multivesicular bodies and late endosomes which inhibits the fusion between virion and endosomal membranes (Amini-Bavil-Olyaee *et al.*, 2013). However, a unifying mechanism to explain antiviral restriction by IFITM proteins remains elusive (Perreira *et al.*, 2013; Smith *et al.*, 2014). Indeed recent reports showing that IFITM3 can be co-opted to promote cell entry of human coronavirus OC43 (Zhao *et al.*, 2014) and human papillomavirus (Warren *et al.*, 2014) suggest virus-specific IFITM interactions.

Although the *IFITM* gene family is evolutionary conserved in vertebrates (Hickford *et al.*, 2012; Zhang *et al.*, 2012), it is unclear whether antiviral activity is also conserved among vertebrate IFITMs. Here, we focused on the bat and pig since these hosts are particularly relevant to the ecology of several IFITM-sensitive zoonotic viruses.

## Results

### Sequence analysis of IFITM3 orthologues cloned from microbat and pig cells

In vertebrates, the *IFITM-1, -2, -3* and *-5* genes cluster together in an *IFITM* locus flanked by the *B4GALNT4* and *ATHL1* genes. It was not possible to assign pig and bat IFITM3 orthologues based on conserved synteny due the lack of a *B4GALNT4* orthologue in pigs, gaps in the genome assemblies, and the low sequencing coverage of the bat genomes (2.6-X for *Pteropus vampyrus* and 1.7-X for *Myotis lucifugus* at the time of analysis). Therefore, to identify *IFITM* genes, rapid amplification of cDNA ends (RACE) was performed on a newborn pig trachea cell line (NPTr) and primary lung fibroblasts from the greater mouse-eared bat, *Myotis myotis*, a European species of microbat (*Vespertilionidae*). *M. myotis* was selected since it is a known reservoir host for several highly pathogenic viruses (Amengual *et al.*, 2007; Drexler *et al.*, 2011; Drexler *et al.*, 2012) and genomes are available for other species from the same genus (Seim *et al.*, 2013; Zhang *et al.*, 2013a).

RACE using primers designed to the conserved central regions of compiled *IFITM*-like sequences yielded several *IFITM* gene variants, of which the designated IFITM3-like sequences were the most abundant. For the pig, the IFITM3-like sequence was the only IFITM variant identified which had an N-terminal extension typical of IFITM2/3 proteins (compare human IFITM1-3 in Fig. 1b). For the microbat, the sequence we assigned as IFITM3 was the most frequent of several long IFITM variants (68% of sequenced clones) and the only one encoding a double phenylalanine motif (F8/F9) conserved in the human and pig IFITM3 orthologues but absent from human IFITM2 (Fig. 1b).

Full-length *IFITM3* cDNA sequences were obtained by RT-PCR, and introns were identified by PCR using genomic DNA, thereby confirming that these are not intron-less expressed

pseudogenes. The transcript structure for pig and microbat IFITM3 was the same as for other experimentally verified IFITM3 orthologues, comprising two exons, a single intron of similar size to other *IFITM3* genes and a conserved exon-exon junction site (Fig. 1a). BLAST searches revealed that the *IFITM3* sequence from NPTr cells is identical to the *Sus scrofa* *IFITM3* reference sequence (NM_001201382.1), and the closest match for the cloned microbat IFITM3 was a 'predicted *IFITM3*-like' gene from *M. lucifugus* (XP_006108229.1, 95% amino acid identity).

Multiple sequence alignments showed that amino acid residues which are functionally important in murine and human IFITM3 are conserved in the cloned pig and microbat orthologues (Fig. 1b). These include (i) three cysteine residues which are S-palmitoylated (Yount *et al.*, 2010), (ii) several lysine residues modified by ubiquitination (Yount *et al.*, 2012) (including K88 which can be monomethylated (Shan *et al.*, 2013)), (iii) the Y20 residue critical for endosomal targeting (Jia *et al.*, 2012; John *et al.*, 2013), (iv) two phenylalanine residues (F75 and F78) which mediate oligomerisation (John *et al.*, 2013) and (v) R85, R87 and Y99 shown to influence antiviral restriction (John *et al.*, 2013). The microbat and pig IFITM3 proteins are most divergent from human IFITM3 at their N and C termini, and most conserved in the central CD225 domain, a pattern shared with other orthologues (chicken and mouse Ifitm3) and paralogues (human IFITM2 and IFITM1) (Fig. 1b).

**Microbat and pig IFITM3 localize to transferrin and CD63 positive endosomes**

To analyse the IFITM3 proteins, A549 cells (which express low levels of endogenous IFITM3 (Brass *et al.*, 2009)) were stably transduced to express C-terminally HA-tagged IFITM3 from pig, microbat or human. Prior work has shown that C-terminal epitope tags do not affect function or expression levels of IFITM3, and indicate that tagged constructs adopt the same topology as the wild type protein (Bailey *et al.*, 2013).

Similar to human IFITM3, both pig and microbat IFITM3 had a punctate intracellular distribution following cell fixation and permeabilisation (Fig. 2a-c) and co-localised with endocytosed transferrin (early endosomes) and with CD63, a marker for late endosomes/ multivesicular bodies (MVBs), but not with the lysosomal marker LAMP1 (Fig 2a-c). There was an enlargement of CD63 positive structures in cells expressing microbat or human IFITM3 in comparison to the smaller CD63 positive vesicles seen in pig IFITM3-expressing or untransduced A549 cells (Fig. 2b). Enlargement of CD63-containing compartments was most marked in cells containing larger foci of IFITM3-HA staining. Microbat IFITM3-HA sometimes co-localised with CD63 in 'hollow' ring-like structures (arrows in Fig. 2b).

**Endocytic uptake of microbat and pig IFITM3 from the plasma membrane**

To investigate the trafficking of pig and microbat IFITM3s, live cells were incubated with FITC-conjugated anti-HA antibody and Alexa 546-conjugated transferrin prior to fixation. When labeling was performed on ice, endocytosis was prevented as indicated by the weak stippled transferrin signal, likely corresponding to clathrin-coated pits pre-internalisation (Fig. 3a). Under these conditions, IFITM3 from the three species was detected on the plasma membrane, clearly highlighting filopodia and membrane ruffles, while no vesicular staining was observed. In contrast, when labeling was performed at 37°C to allow endocytosis, anti-HA staining showed that pig, microbat and human IFITM3 formed discrete puncta, which, as previously observed, overlapped or were closely associated with transferrin-positive endosomes (Fig. 3b). For all IFITM3s, internalization of the anti-HA antibody by live cells identified larger, brighter puncta that were more widely distributed within the cytosol compared to the HA staining seen previously following fixation and permeabilisation (indicating that permeabilisation may cause some extraction of the membrane associated IFITM3). In conclusion, pig and microbat IFITM3 share the following with their human counterpart: (i) plasma membrane trafficking (ii) extracellular exposure of their C-termini

(allowing detection of the C-terminal HA tag in intact cells) and (iii) endocytic uptake from the plasma membrane into the endosomal pathway.

**Microbat and pig IFITM3 restrict cell entry mediated by influenza HA**

To determine whether pig and microbat IFITM3 restrict influenza A virus entry, lentiviruses expressing the HA proteins from diverse influenza subtypes were used to infect A549 cells that were untransduced or had been transduced to express either human IFITM3, pig IFITM3 (Fig. 4a) or microbat IFITM3 (Fig. 4b). Three independently cloned cell lines of the pig and microbat IFITM3s markedly inhibited the infectivity of all influenza HA subtypes tested, including both Group I and Group 2 HAs and highly pathogenic avian H5 and H7 (Fig. 4). Pig or microbat IFITM3 did not restrict viruses pseudotyped with the entry proteins of the gammaretroviruses amphotrophic murine leukemia virus or Gibbon ape leukemia virus (Fig. S1), consistent with previous studies on human IFITM3 (Brass *et al.*, 2009; Huang *et al.*, 2011).

**Microbat and pig IFITM3 inhibit replication-competent influenza virus**

To assess the effect of the IFITM3 orthologues on replication-competent influenza virus, untransduced A549 cells or cells expressing either human, pig or microbat IFITM3 were infected with influenza A/WSN/33 (H1N1) and nucleoprotein (NP) expression was quantitated using flow cytometry. Expression of either pig or microbat IFITM3 led to a marked reduction in the proportion of NP positive cells for all cell clones (Fig. 5a). There was slight variation in the degree of restriction between the three cell lines expressing pig IFITM3 (Fig. 5a and Fig. S2) despite comparable expression of IFITM3-HA seen by Western blot (Fig. S2).

Stable expression of either pig, microbat or human IFITM3 in A549 cells significantly reduced single cycle growth of influenza A/WSN/33 (Fig. 5c), consistent with reduced NP expression measured in parallel (Fig 5b). Inhibition of virus yields was more profound following low m.o.i. infection (>1 $\log_{10}$ for pig IFITM3 and >2 $\log_{10}$ for both microbat and human IFITM3) relative to control GFP-expressing cells (Fig. 5d). A similar pattern of restriction was also observed when NP expression was analysed after infections with an avian-like swine influenza strain, A/swine/453/06 (H1N1) (Fig. 5b). Levels of the stably expressed proteins were examined by Western blotting against the C–terminal HA epitope tag, and showed that pig IFITM3, human IFITM3 and GFP-HA expression were comparable while microbat IFITM3 was more highly expressed (Fig. 5c and Fig S3).

**Microbat and pig IFITM3 block cell entry mediated by lyssavirus entry proteins**

In light of data which suggest there may be virus-specific antiviral determinants of IFITM (John *et al.*, 2013; Zhao *et al.*, 2014), it was of interest to explore the antiviral spectrum of pig and microbat IFITM3, especially for viruses that naturally infect these species.

A549 cells stably expressing either pig, microbat or human IFITM3 were infected with pseudotyped lentiviruses that expressed the envelope glycoproteins from isolates representing different lyssavirus phylogroups, namely the rabies virus strain Evelyn Rokitniki Abelseth (phylogroup 1), Mokola virus (phylogroup 2), Lagos bat virus (phylogroup 2) and West Caucasian bat virus (phylogroup 3). Expression of IFITM3 from either microbat, pig or human reduced infectivity mediated by all four lyssavirus entry proteins, in all cases by approximately 2 $\log_{10}$ relative to control cells (Fig. 6). Thus, the pig and microbat IFITM3 orthologues inhibit cell entry mediated by multiple lyssavirus G proteins.

**IFITM3 activity in pig and microbat cells**

Finally, we addressed the contribution of IFITM3 to antiviral responses in pig and microbat cells. Endogenous IFITM3 expression was measured using Taqman qRT-PCR designed to specifically detect IFITM3 mRNA and not other IFITM paralogues identified in these cells by RACE. Baseline levels of IFITM3 mRNA were readily detected in both the porcine NPTr cells (Ct value IFITM3: 22.7; Ct value GAPDH 21.33) and in microbat lung fibroblasts (Ct value IFITM3: 25.8; Ct value GAPDH 22.8). IFITM3 induction was assessed in response to the dsRNA analogue polyI:C, a molecular pattern associated with viral infection which is recognised by toll-like receptor 3 and induces Type I IFN in porcine (Provost *et al.*, 2012) and bat cells (Biesold *et al.*, 2011; Omatsu *et al.*, 2008; Zhou *et al.*, 2011). PolyI:C addition led to a 3.5-fold increase in pig IFITM3 and a 2-fold increase in microbat IFITM3 mRNA levels (Fig. 7). The microbat cells were also stimulated via polyI:C transfection since in pteropid bat lung cells (but not primary cells from other tissues) this enhanced IFNβ induction relative to extracellular delivery of polyI:C (Zhou *et al.*, 2011). However, transfection of polyI:C into microbat cells resulted in a similar degree of IFITM3 induction (2.3-fold) (Fig. 7).

Next, the function of endogenous IFITM3 was assessed using siRNA designed using the RACE sequence data to target IFITM3 and not other putative IFITM paralogues. siRNA targeting IFITM3 or control non-targeting siRNAs were transfected into cells with polyI:C induction of IFITM3. IFITM3 mRNA was quantified by qRT-PCR and the biological effect of the knockdown assessed by infection with influenza A/WSN/33 (Fig. 8). Transfection of siRNA against pig IFITM3 led to a 63% knockdown in IFITM3 mRNA (1.4 $\log_2$ fold change) (Fig. 8a), a 3.4-fold increase in virus yields (Fig. 8b) and a 2-fold increase in the proportion of influenza NP positive cells (Fig. 8c) relative to control siRNA transfected cells. In the absence of polyI:C stimulation, IFITM3 knockdown in NPTr cells increased influenza NP positive cells more (3.3-fold) (Fig. 8d) suggesting additional polyI:C induced genes complement IFITM3 mediated influenza virus restriction. Microbat IFITM3 knockdown in the absence of polyI:C stimulation (Fig. 8e-g) reduced IFITM3 mRNA levels by 60% (1.3 $\log_2$ fold

change) (Fig. 8e) and led to a 2-fold increase in infectious yields (Fig. 8f) and a 3-fold increase in NP expression (Fig. 8g), relative to control siRNA transfection. Thus, endogenous IFITM3 in pig tracheal NPTr cells and microbat lung cells restricts influenza virus. Lastly, following siRNA knockdown of baseline IFITM3 in a microbat cell line, overexpression of microbat IFITM3 significantly inhibited influenza NP expression (Fig. S4).

## Discussion

Species differences in restriction factors can determine differential viral susceptibility (Duggal & Emerman, 2012; Fadel & Poeschla, 2011; Kirmaier *et al.*, 2010; McNatt *et al.*, 2009). However, antiviral immunity in reservoir and spill-over hosts remains poorly understood, although important for understanding viral emergence (Bean *et al.*, 2013). Here we show that IFITM3 proteins with broad-spectrum antiviral function are conserved in swine and Chiroptera, hosts of numerous zoonotic viruses.

The RACE reactions used here capture multiple possible expressed IFITM paralogues by using primers against the conserved CD225 domain. We assigned microbat IFITM3 using several criteria. First, it encodes a double phenylalanine motif (F8/F9) found only in other IFITM3 orthologues (whereas the other microbat IFITM variants resembled human IFITM2 in having a single phenylalanine at this position). Secondly, microbat IFITM3 had an intracellular location and co-localised with endosomal markers. Conserved genome synteny was previously used to help assign IFITM genes (Smith *et al.*, 2013; Zhang *et al.*, 2012), but was of limited use in the case of the poorly assembled IFITM loci in the pig and microbat genomes. Moreover, the IFITM gene family is associated with numerous processed pseudogenes, gene duplications and copy number variation (Siegrist *et al.*, 2011; Zhang *et al.*, 2012), which significantly complicates the assignment of gene orthology. Although, a recent computational study identified 8 pig IFITM family members with expressed sequence tag (EST) evidence (Miller *et al.*, 2014), it lacked the functional validation presented here.

Functionally important amino acid residues for human or mouse IFITM3 were conserved in pig and microbat IFITM3, indicating that these may be functionally important sites across the orthologues. Amino acid residues are less conserved within IM2 compared to IM1, although IM2 can function as a signal anchor for membrane localisation (Bailey *et al.*, 2013) and is also sufficient to mediate the IFITM3-VAPA interaction (Amini-Bavil-Olyaee *et al.*, 2013).

We show here that C-terminally HA-tagged IFITM3 (of human, pig and microbat) was clearly detectable at the plasma membrane after live cell staining. These data support recent evidence for a luminal (i.e. extracellular) exposure of the C-terminus (Bailey *et al.*, 2013), and indicate that pig and microbat IFITM3 adopt a similar topology. Other studies have also reported that a proportion of human IFITM3 localises to the plasma membrane (Amini-Bavil-Olyaee *et al.*, 2013; Bailey *et al.*, 2013; Brass *et al.*, 2009), and it is thought that the 20-YEML-23 motif acts as a lysosomal sorting signal for the internalisation of IFITM3 into the endosomal pathway (Jia *et al.*, 2012; John *et al.*, 2013). Pig and microbat IFITM3 contain 20-YEML-23 and 20-YEVL-23 respectively (which conform to the consensus sequence for a tyrosine-based sorting signal YxxΦ, where Φ is a residue with a bulky hydrophobic side chain (Bonifacino & Traub, 2003)), and likewise were observed to traffic into endosomes following their cell surface staining. Pig and microbat IFITM3 co-localised with endocytosed transferrin (early endosomes) and CD63 (late endosomes/ MVBs) as seen for human IFITM3 (Figs. 2 and 3 and (Amini-Bavil-Olyaee *et al.*, 2013; Feeley *et al.*, 2011; Huang *et al.*, 2011; Jia *et al.*, 2012; Lu *et al.*, 2011). Expression of both microbat and human IFITM3 caused expansion of CD63 positive endosomal compartments, consistent with the documented ability of IFITM3 to induce MVB formation (Amini-Bavil-Olyaee *et al.*, 2013). Furthermore, in some cells microbat IFITM3 co-stained with CD63 in ring-like structures, a phenomenon reported for human IFITM3 and enhanced by overexpression of its interaction partner VAPA (Amini-Bavil-Olyaee *et al.*, 2013). In our hands neither human IFITM3 nor its pig and microbat orthologues co-localised with the lysosomal marker LAMP1, which is consistent with some (Yount *et al.*, 2010) but not other (Feeley *et al.*, 2011; Huang *et al.*,

2011) reports for IFITM3 localisation. These discrepancies regarding localisation may be due to IFITM3's multiple post-translational modifications (Yount *et al.*, 2012) and/or cell type-dependent differences in its topology (Bailey *et al.*, 2013).

We show that both pig and microbat IFITM3 restrict cell entry mediated by multiple influenza A virus HA (a class I fusion protein) and lyssavirus G proteins (a class III fusion protein). Restriction at the level of cell entry correlated with significant inhibition of influenza virus yields and NP expression. The microbat, pig and human IFITM3-expressing A549 cells varied in their IFITM3 expression levels, which may underlie variation seen in the degree of restriction. However, anti-influenza restriction by pig IFITM3 was in general lower than that seen for human IFITM3, despite comparable expression levels. We found that pig and human IFITM3 can restrict avian, swine and human influenza A subtypes. Similarly, chicken IFITM3 inhibited viral pseudotypes bearing HAs from both avian and human strains (Smith *et al.*, 2013). siRNA knockdown of endogenous pig and microbat IFITM3 enhanced influenza replication by a similar degree to that seen following knockdown of human IFITM3 (Huang *et al.*, 2011) or chicken IFITM3 (Smith *et al.*, 2013). IFITM3 was constitutively expressed in pig and bat cells (as reported for other IFITM3 orthologues (Bailey *et al.*, 2012; Everitt *et al.*, 2013; Everitt *et al.*, 2012; Friedman *et al.*, 1984; Smith *et al.*, 2013)). Baseline levels of IFITM3 in the pig and bat cells were sufficient to limit viral replication and, following siRNA targeting of baseline IFITM3, microbat IFITM3 was also capable of restricting influenza virus when overexpressed in microbat cells. Since pig IFITM3 was moderately induced by polyI:C and up-regulated upon viral challenge *in vivo* (Andersson *et al.*, 2011; Miller *et al.*, 2014), pig IFITM3 is likely to be relevant to host antiviral responses.

Here, we show that influenza A viruses and lysssaviruses, virus families which share an ancient co-evolutionary history with bats (Badrane & Tordo, 2001; Tong *et al.*, 2013) are restricted by microbat IFITM3. Bats harbour many diverse virus types and are important reservoirs of zoonotic infections (Drexler *et al.*, 2014; Quan *et al.*, 2013; Smith & Wang,

2013; Tong *et al.*, 2013). However, the basis for the intimate association between bats and viruses remains enigmatic, particularly the relative importance of immunological compared to ecological or life history factors (Kupferschmidt, 2013). Although transcriptional induction of chiropteran ISG orthologues is reported (Papenfuss *et al.*, 2012; Zhou *et al.*, 2013), there is a striking lack of functional data for any of these genes. We demonstrate that bats do encode functional IFITM3 and therefore are likely to be competent in this aspect of intrinsic antiviral restriction.

## Methods

### Cells

A549 cells were maintained in F12 medium, and 293T, NPTr cells (Ferrari *et al.*, 2003) and FLN-R cells (Cat No. CCLV-RIE 1091 (Friedrich-Loeffler-Institut, Greifswald-Insel Riems, Germany) were grown in DMEM with 10% FCS. Primary lung cells from the microbat *Myotis myotis* were grown in DMEM containing 10% FCS, penicillin and streptomycin and 20% amnioMAX (Gibco).

### RACE & IFITM3 cloning

NPTr and microbat cells were transfected with polyI:C (Invivogen, tlrl-pic) at 33ug/ml using Lipofectamine 2000 and 4h later total RNA and genomic DNA were isolated (Qiagen AllPrep Kit). 5' and 3' IFITM cDNA fragments were generated using the SMARTer RACE cDNA amplification kit (Clontech) and the following primers (designated by name): '5Bat': gcccagagctatgcgtccaccgccaagtgcc; '3Bat': cgtctggtccctgttcaacaccctcttc; '5Pig': gatgttcaggcacttggcggtggaggcatagctc; '3Pig': tgaactggtgctgcctgggcttcgtgg. PCR products were TA cloned and multiple clones sequenced using Sanger sequencing. Non-coding sequences identified by RACE were used to design primers for PCR amplification of full length IFITM3 ('BatIFITM3ncrF': gcatccacacgccatctgctc; 'BatIFITM3ncrR':

gaacgccattgtgcacatgtgc; ‘PigIFITM3ncrF’: acagcttctcctgggcaccatg; ‘PigIFITM3ncrR’: gtatgtgctgctgtgaaaggag). Pig IFITM3 and microbat IFITM3 were synthesized as codon-optimised genes for expression in human cells (GeneArt) and cloned into the BamHI and NotI sites of the lentivirus vector pSIN-BNHA (derived from pHRSIN-CSGW (Demaison *et al.*, 2002)).

**Creation of IFITM3-expressing cell lines**

Lentiviruses expressing IFITM3 (or GFP as a control) were produced by co-transfecting 293T cells using Fugene HD with the packaging plasmid p8.91 (Zufferey *et al.*, 1997) (1ug), the VSV-G expressing plasmid pMDG (1ug) and the lentivirus vector pSIN-BNHA (1.5ug) containing either pig IFITM3, microbat IFITM3 or GFP. Supernatants were harvested at 48h and 72h, filtered (0.45um) and used to transduce A549 cells. Transduction efficiency was checked after 48h via flow cytometric detection of HA. Single cell clones were generated using limiting dilution and analysed for HA expression. Those with the most similar expression levels were selected for experiments. Human IFITM3-expressing A549 cells were generated using the same method (Smith *et al.*, 2013).

**Pseudotyped lentivirus cell entry assay**

Lentiviral pseudotypes were produced as previously (Ferrara *et al.*, 2012; Wright *et al.*, 2008). For the entry assay, A549 cells were seeded in white 96 well plates (1e4 cells/ well) one day prior to infection with luciferase-expressing pseudotypes expressing influenza hemagglutinin (HA) (H1: GenBank accession AAD17229.1; H5: ABP51969.1; H10: ABI84534.1; H14: BAF43460.1; H7: CAD37074.1; H3: AAA43099.1; H15: AAA96134.1), the G proteins from Mokola virus (MOKV.98/071 RA361: GQ500108), Lagos Bat Virus (LBV.NIG56-RV1: HM623779), West Caucasian Bat Virus (WCBV: AAR03484) or Evelyn Rokitniki Abelseth rabies strain (ERA: ABN11294) or MLV-A or GALV envelope proteins. The H1 and H3 HAs were human in origin, and the other HA subtypes were avian in origin.

Cells were infected in triplicate and 48h later luciferase activity was measured using the Bright Glo luciferase assay system (Promega).

**siRNA transfection and Real-Time PCR**

siRNAs against pig IFITM3 (GCTCATAAAGGATTACAGA) or microbat IFITM3 (CGAGGACGACGGTGGTCAA) (Dharmacon, ON-TARGETplus) were designed using knowledge of other IFITM paralogues and the Dharmacon siDesign Centre. The ON-TARGETplus non-targeting siRNA pool and an siRNA targeting GFP (P-002048-01-20) were used as controls. siRNA was transfected into cells (20pmol per well of a 12 well plate) using Lipofectamine RNAiMAX. 48h later, RNA was extracted (RNeasy kit, Qiagen) and the Quantitect multiplex RT-PCR kit (Qiagen) was used to measure IFITM3 and GAPDH simultaneously using TaqMan gene expression assays (Applied biosystems, primer sequences available on request). MxPro software was used for comparative quantitation of IFITM3 relative to the GAPDH reference gene.

**Flow cytometry**

Cells were infected in triplicate with influenza A/WSN/33 in media containing 2% FCS. Cells were trypsinised, fixed using BD Fixation/Permeabilisation solution for 20 min and washed twice in BD Perm/Wash buffer before incubation with FITC-conjugated anti-influenza NP IgG (Abcam ab20921) for 40 min at 4 $^{o}$C. After staining, cells were washed, resuspended in PBS and analysed using a Becton Dickinson FACSCalibur and Cell Quest Pro. For each sample, 10,000 cells (gated by forward and side scatter) were analysed for FITC fluorescence.

**Western blotting**

After cell lysis using RIPA buffer, proteins were separated by SDS-PAGE (4-12% TGX gel) and transferred to nitrocellulose membrane. After blocking (5% Marvel, 0.1% Tween-20 in PBS), membranes were incubated for 1h at room temperature with antibodies against influenza NP (Abcam clone C43), beta-actin (Abcam ab8227) or the HA tag (Abcam clone

HA.C5). HRP-conjugated secondary antibodies were used followed by enhanced chemiluminescent detection.

**Virus yield assay**

Cells were infected in triplicate with influenza A/WSN/33 in media containing 2% FCS. After 1h infection at 37$^{o}$C, cells were washed thrice in PBS. At the indicated times post infection, supernatants were harvested and the virus yields titered on MDCK cells by plaque assay (Matrosovich *et al.*, 2006).

**Immunofluorescence**

Cells were fixed with 4% paraformaldehyde (20 min at room temperature). For transferrin co-localisation, cells were pre-incubated with Alexa 546-conjugated transferrin (Molecular Probes, 5ug/ml) for 10 min before fixation. Cells were permeabilised using 0.2% Triton X-100, blocked using antibody buffer (0.1% Tween 20 and 10% goat serum in PBS) and stained with FITC-conjugated anti-HA (Bethyl Laboratories A190-108F), anti-LAMP1 (Abcam clone H4A3) or anti-CD63 (Santa Cruz MX-49.129.5) for 1 h at room temperature. Dylight 594-conjugated goat anti-mouse IgG was used to detect anti-CD63 and anti-LAMP1 antibodies. Live cell staining was performed either at 37$^{o}$C or on ice, with solutions equilibrated accordingly. Cells were washed twice in serum-free media before incubation for 30 min with FITC conjugated anti-HA and Alexa 546-conjugated transferrin (in serum free media). Cells were then quickly washed in PBS and immediately fixed using 4% paraformaldehyde (20 min). Coverslips were mounted using ProLong Gold reagent with DAPI and examined with a Zeiss LSM 780 confocal microscope.

**Sequence analysis**

Multiple sequence alignments were performed using Clustal O (1.2.0) and Seaview (Gouy *et al.*, 2010) was used for manual editing.

**Acknowledgements**

This work was supported by an award to C. Benfield from the Royal Veterinary College Internal Grant Scheme (IGS 2930) and by the Wellcome Trust grant (098051) and the MRC grant (G1000413).

We are grateful to Prof Malcolm Ferguson-Smith for supplying the primary bat cells, to Prof Martin Beer (Friedrich-Loeffler-Institut) for providing FLN-R cells, to Prof Wendy Barclay for supplying influenza virus, to Dr Fengtang Yang and Beiyuan Fu for their assistance with primary cell culture, to Dr Mike Hollinshead for microscopy support, to Dr Matt Cotten and Dr Simon Watson for bioinformatics assistance and to Dr Laurence Tiley, Dr Barbara Blacklaws and Dr Dirk Werling for helpful discussions.

## REFERENCES


**Amengual, B., Bourhy, H., Lopez-Roig, M. & Serra-Cobo, J. (2007).** Temporal dynamics of European bat Lyssavirus type 1 and survival of Myotis myotis bats in natural colonies. *PLoS One* **2**, e566.

**Amini-Bavil-Olyaee, S., Choi, Y. J., Lee, J. H., Shi, M., Huang, I. C., Farzan, M. & Jung, J. U. (2013).** The antiviral effector IFITM3 disrupts intracellular cholesterol homeostasis to block viral entry. *Cell host & microbe* **13**, 452-464.

**Anafu, A. A., Bowen, C. H., Chin, C. R., Brass, A. L. & Holm, G. H. (2013).** Interferon-inducible transmembrane protein 3 (IFITM3) restricts reovirus cell entry. *The Journal of biological chemistry* **288**, 17261-17271.

**Andersson, M., Ahlberg, V., Jensen-Waern, M. & Fossum, C. (2011).** Intestinal gene expression in pigs experimentally co-infected with PCV2 and PPV. *Veterinary immunology and immunopathology* **142**, 72-80.

**Badrane, H. & Tordo, N. (2001).** Host switching in Lyssavirus history from the Chiroptera to the Carnivora orders. *J Virol* **75**, 8096-8104.

**Bailey, C. C., Huang, I. C., Kam, C. & Farzan, M. (2012).** Ifitm3 limits the severity of acute influenza in mice. *PLoS Pathog* **8**, e1002909.

**Bailey, C. C., Kondur, H. R., Huang, I. C. & Farzan, M. (2013).** Interferon-induced transmembrane protein 3 is a type II transmembrane protein. *The Journal of biological chemistry* **288**, 32184-32193.

**Bean, A. G., Baker, M. L., Stewart, C. R., Cowled, C., Deffrasnes, C., Wang, L. F. & Lowenthal, J. W. (2013).** Studying immunity to zoonotic diseases in the natural host - keeping it real. *Nature reviews Immunology* **13**, 851-861.

**Biesold, S. E., Ritz, D., Gloza-Rausch, F., Wollny, R., Drexler, J. F., Corman, V. M., Kalko, E. K., Oppong, S., Drosten, C. & other authors (2011).** Type I interferon reaction to viral infection in interferon-competent, immortalized cell lines from the African fruit bat Eidolon helvum. *PLoS One* **6**, e28131.

**Bonifacino, J. S. & Traub, L. M. (2003).** Signals for sorting of transmembrane proteins to endosomes and lysosomes. *Annual review of biochemistry* **72**, 395-447.

**Brass, A. L., Huang, I. C., Benita, Y., John, S. P., Krishnan, M. N., Feeley, E. M., Ryan, B. J., Weyer, J. L., van der Weyden, L. & other authors (2009).** The IFITM proteins mediate cellular resistance to influenza A H1N1 virus, West Nile virus, and dengue virus. *Cell* **139**, 1243-1254.

**Chen, Y. X., Welte, K., Gebhard, D. H. & Evans, R. L. (1984).** Induction of T cell aggregation by antibody to a 16kd human leukocyte surface antigen. *J Immunol* **133**, 2496-2501.

**Demaison, C., Parsley, K., Brouns, G., Scherr, M., Battmer, K., Kinnon, C., Grez, M. & Thrasher, A. J. (2002).** High-level transduction and gene expression in hematopoietic repopulating cells using a human immunodeficiency [correction of imunodeficiency] virus type 1-based lentiviral vector containing an internal spleen focus forming virus promoter. *Human gene therapy* **13**, 803-813.

**Drexler, J. F., Corman, V. M. & Drosten, C. (2014).** Ecology, evolution and classification of bat coronaviruses in the aftermath of SARS. *Antiviral research* **101**, 45-56.

**Drexler, J. F., Corman, V. M., Wegner, T., Tateno, A. F., Zerbinati, R. M., Gloza-Rausch, F., Seebens, A., Muller, M. A. & Drosten, C. (2011).** Amplification of emerging viruses in a bat colony. *Emerging infectious diseases* **17**, 449-456.

552 **Drexler, J. F., Corman, V. M., Muller, M. A., Maganga, G. D., Vallo, P., Binger, T., Gloza-Rausch, F., Rasche, A., Yordanov, S. & other authors (2012).** Bats host major mammalian paramyxoviruses. *Nat Commun* **3**, 796.
555 **Duggal, N. K. & Emerman, M. (2012).** Evolutionary conflicts between viruses and restriction factors shape immunity. *Nature reviews Immunology* **12**, 687-695.
557 **Everitt, A. R., Clare, S., McDonald, J. U., Kane, L., Harcourt, K., Ahras, M., Lall, A., Hale, C., Rodgers, A. & other authors (2013).** Defining the range of pathogens susceptible to Ifitm3 restriction using a knockout mouse model. *PLoS One* **8**, e80723.
561 **Everitt, A. R., Clare, S., Pertel, T., John, S. P., Wash, R. S., Smith, S. E., Chin, C. R., Feeley, E. M., Sims, J. S. & other authors (2012).** IFITM3 restricts the morbidity and mortality associated with influenza. *Nature* **484**, 519-523.
564 **Fadel, H. J. & Poeschla, E. M. (2011).** Retroviral restriction and dependency factors in primates and carnivores. *Veterinary immunology and immunopathology* **143**, 179-189.
567 **Feeley, E. M., Sims, J. S., John, S. P., Chin, C. R., Pertel, T., Chen, L. M., Gaiha, G. D., Ryan, B. J., Donis, R. O. & other authors (2011).** IFITM3 inhibits influenza A virus infection by preventing cytosolic entry. *PLoS Pathog* **7**, e1002337.
570 **Ferrara, F., Molesti, E., Bottcher-Friebertshauser, E., Cattoli, G., Corti, D., Scott, S. D. & Temperton, N. J. (2012).** The human Transmembrane Protease Serine 2 is necessary for the production of Group 2 influenza A virus pseudotypes. *Journal of molecular and genetic medicine : an international journal of biomedical research* **7**, 309-314.
575 **Ferrari, M., Scalvini, A., Losio, M. N., Corradi, A., Soncini, M., Bignotti, E., Milanesi, E., Ajmone-Marsan, P., Barlati, S. & other authors (2003).** Establishment and characterization of two new pig cell lines for use in virological diagnostic laboratories. *Journal of virological methods* **107**, 205-212.
579 **Friedman, R. L., Manly, S. P., McMahon, M., Kerr, I. M. & Stark, G. R. (1984).** Transcriptional and posttranscriptional regulation of interferon-induced gene expression in human cells. *Cell* **38**, 745-755.
582 **Gouy, M., Guindon, S. & Gascuel, O. (2010).** SeaView version 4: A multiplatform graphical user interface for sequence alignment and phylogenetic tree building. *Molecular biology and evolution* **27**, 221-224.
585 **Hickford, D., Frankenberg, S., Shaw, G. & Renfree, M. B. (2012).** Evolution of vertebrate interferon inducible transmembrane proteins. *BMC Genomics* **13**, 155.
587 **Huang, I. C., Bailey, C. C., Weyer, J. L., Radoshitzky, S. R., Becker, M. M., Chiang, J. J., Brass, A. L., Ahmed, A. A., Chi, X. & other authors (2011).** Distinct patterns of IFITM-mediated restriction of filoviruses, SARS coronavirus, and influenza A virus. *PLoS Pathog* **7**, e1001258.
591 **Jia, R., Pan, Q., Ding, S., Rong, L., Liu, S. L., Geng, Y., Qiao, W. & Liang, C. (2012).** The N-terminal region of IFITM3 modulates its antiviral activity by regulating IFITM3 cellular localization. *J Virol* **86**, 13697-13707.
594 **John, S. P., Chin, C. R., Perreira, J. M., Feeley, E. M., Aker, A. M., Savidis, G., Smith, S. E., Elia, A. E., Everitt, A. R. & other authors (2013).** The CD225 domain of IFITM3 is required for both IFITM protein association and inhibition of influenza A virus and dengue virus replication. *J Virol* **87**, 7837-7852.
598 **Kirmaier, A., Wu, F., Newman, R. M., Hall, L. R., Morgan, J. S., O'Connor, S., Marx, P. A., Meythaler, M., Goldstein, S. & other authors (2010).** TRIM5 suppresses

cross-species transmission of a primate immunodeficiency virus and selects for emergence of resistant variants in the new species. *PLoS biology* **8**.

**Kupferschmidt, K. (2013).** Emerging infectious diseases. Link to MERS virus underscores bats' puzzling threat. *Science* **341**, 948-949.

**Li, K., Markosyan, R. M., Zheng, Y. M., Golfetto, O., Bungart, B., Li, M., Ding, S., He, Y., Liang, C. & other authors (2013).** IFITM proteins restrict viral membrane hemifusion. *PLoS Pathog* **9**, e1003124.

**Lu, J., Pan, Q., Rong, L., He, W., Liu, S. L. & Liang, C. (2011).** The IFITM proteins inhibit HIV-1 infection. *J Virol* **85**, 2126-2137.

**Matrosovich, M., Matrosovich, T., Garten, W. & Klenk, H. D. (2006).** New low-viscosity overlay medium for viral plaque assays. *Virology journal* **3**, 63.

**McNatt, M. W., Zang, T., Hatziioannou, T., Bartlett, M., Fofana, I. B., Johnson, W. E., Neil, S. J. & Bieniasz, P. D. (2009).** Species-specific activity of HIV-1 Vpu and positive selection of tetherin transmembrane domain variants. *PLoS Pathog* **5**, e1000300.

**Miller, L. C., Jiang, Z., Sang, Y., Harhay, G. P. & Lager, K. M. (2014).** Evolutionary characterization of pig interferon-inducible transmembrane gene family and member expression dynamics in tracheobronchial lymph nodes of pigs infected with swine respiratory disease viruses. *Veterinary immunology and immunopathology* **159**, 180-191.

**Moffatt, P., Gaumond, M. H., Salois, P., Sellin, K., Bessette, M. C., Godin, E., de Oliveira, P. T., Atkins, G. J., Nanci, A. & other authors (2008).** Bril: a novel bone-specific modulator of mineralization. *Journal of bone and mineral research : the official journal of the American Society for Bone and Mineral Research* **23**, 1497-1508.

**Mudhasani, R., Tran, J. P., Retterer, C., Radoshitzky, S. R., Kota, K. P., Altamura, L. A., Smith, J. M., Packard, B. Z., Kuhn, J. H. & other authors (2013).** IFITM-2 and IFITM-3 but not IFITM-1 restrict Rift Valley fever virus. *J Virol* **87**, 8451-8464.

**Omatsu, T., Bak, E. J., Ishii, Y., Kyuwa, S., Tohya, Y., Akashi, H. & Yoshikawa, Y. (2008).** Induction and sequencing of Rousette bat interferon alpha and beta genes. *Veterinary immunology and immunopathology* **124**, 169-176.

**Papenfuss, A. T., Baker, M. L., Feng, Z. P., Tachedjian, M., Crameri, G., Cowled, C., Ng, J., Janardhana, V., Field, H. E. & other authors (2012).** The immune gene repertoire of an important viral reservoir, the Australian black flying fox. *BMC Genomics* **13**, 261.

**Perreira, J. M., Chin, C. R., Feeley, E. M. & Brass, A. L. (2013).** IFITMs Restrict the Replication of Multiple Pathogenic Viruses. *Journal of molecular biology* **425**, 4937-4955.

**Provost, C., Jia, J. J., Music, N., Levesque, C., Lebel, M. E., del Castillo, J. R., Jacques, M. & Gagnon, C. A. (2012).** Identification of a new cell line permissive to porcine reproductive and respiratory syndrome virus infection and replication which is phenotypically distinct from MARC-145 cell line. *Virology journal* **9**, 267.

**Quan, P. L., Firth, C., Conte, J. M., Williams, S. H., Zambrana-Torrelio, C. M., Anthony, S. J., Ellison, J. A., Gilbert, A. T., Kuzmin, I. V. & other authors (2013).** Bats are a major natural reservoir for hepaciviruses and pegiviruses. *Proceedings of the National Academy of Sciences of the United States of America* **110**, 8194-8199.

**Seim, I., Fang, X., Xiong, Z., Lobanov, A. V., Huang, Z., Ma, S., Feng, Y., Turanov, A. A., Zhu, Y. & other authors (2013).** Genome analysis reveals insights into physiology and longevity of the Brandt's bat Myotis brandtii. *Nat Commun* **4**, 2212.

**Shan, Z., Han, Q., Nie, J., Cao, X., Chen, Z., Yin, S., Gao, Y., Lin, F., Zhou, X. & other authors (2013).** Negative Regulation of Interferon-induced Transmembrane Protein 3 by SET7-mediated Lysine Monomethylation. *The Journal of biological chemistry* **288**, 35093-35103.

**Siegrist, F., Ebeling, M. & Certa, U. (2011).** The small interferon-induced transmembrane genes and proteins. *Journal of interferon & cytokine research : the official journal of the International Society for Interferon and Cytokine Research* **31**, 183-197.

**Smith, I. & Wang, L. F. (2013).** Bats and their virome: an important source of emerging viruses capable of infecting humans. *Current opinion in virology* **3**, 84-91.

**Smith, S., Weston, S., Kellam, P. & Marsh, M. (2014).** IFITM proteins-cellular inhibitors of viral entry. *Current opinion in virology* **4C**, 71-77.

**Smith, S. E., Gibson, M. S., Wash, R. S., Ferrara, F., Wright, E., Temperton, N., Kellam, P. & Fife, M. (2013).** Chicken interferon-inducible transmembrane protein 3 restricts influenza viruses and lyssaviruses in vitro. *J Virol* **87**, 12957-12966.

**Takahashi, S., Doss, C., Levy, S. & Levy, R. (1990).** TAPA-1, the target of an antiproliferative antibody, is associated on the cell surface with the Leu-13 antigen. *J Immunol* **145**, 2207-2213.

**Tong, S., Zhu, X., Li, Y., Shi, M., Zhang, J., Bourgeois, M., Yang, H., Chen, X., Recuenco, S. & other authors (2013).** New world bats harbor diverse influenza A viruses. *PLoS Pathog* **9**, e1003657.

**Wang, Z., Zhang, A., Wan, Y., Liu, X., Qiu, C., Xi, X., Ren, Y., Wang, J., Dong, Y. & other authors (2014).** Early hypercytokinemia is associated with interferon-induced transmembrane protein-3 dysfunction and predictive of fatal H7N9 infection. *Proceedings of the National Academy of Sciences of the United States of America* **111**, 769-774.

**Warren, C. J., Griffin, L. M., Little, A. S., Huang, I. C., Farzan, M. & Pyeon, D. (2014).** The Antiviral Restriction Factors IFITM1, 2 and 3 Do Not Inhibit Infection of Human Papillomavirus, Cytomegalovirus and Adenovirus. *PLoS One* **9**, e96579.

**Weidner, J. M., Jiang, D., Pan, X. B., Chang, J., Block, T. M. & Guo, J. T. (2010).** Interferon-induced cell membrane proteins, IFITM3 and tetherin, inhibit vesicular stomatitis virus infection via distinct mechanisms. *J Virol* **84**, 12646-12657.

**Wright, E., Temperton, N. J., Marston, D. A., McElhinney, L. M., Fooks, A. R. & Weiss, R. A. (2008).** Investigating antibody neutralization of lyssaviruses using lentiviral pseudotypes: a cross-species comparison. *J Gen Virol* **89**, 2204-2213.

**Yount, J. S., Karssemeijer, R. A. & Hang, H. C. (2012).** S-palmitoylation and ubiquitination differentially regulate interferon-induced transmembrane protein 3 (IFITM3)-mediated resistance to influenza virus. *The Journal of biological chemistry* **287**, 19631-19641.

**Yount, J. S., Moltedo, B., Yang, Y. Y., Charron, G., Moran, T. M., Lopez, C. B. & Hang, H. C. (2010).** Palmitoylome profiling reveals S-palmitoylation-dependent antiviral activity of IFITM3. *Nature chemical biology* **6**, 610-614.

**Zhang, G., Cowled, C., Shi, Z., Huang, Z., Bishop-Lilly, K. A., Fang, X., Wynne, J. W., Xiong, Z., Baker, M. L. & other authors (2013a).** Comparative analysis of bat

genomes provides insight into the evolution of flight and immunity. *Science* **339**, 456-460.

**Zhang, Y. H., Zhao, Y., Li, N., Peng, Y. C., Giannoulatou, E., Jin, R. H., Yan, H. P., Wu, H., Liu, J. H. & other authors (2013b).** Interferon-induced transmembrane protein-3 genetic variant rs12252-C is associated with severe influenza in Chinese individuals. *Nat Commun* **4**, 1418.

**Zhang, Z., Liu, J., Li, M., Yang, H. & Zhang, C. (2012).** Evolutionary dynamics of the interferon-induced transmembrane gene family in vertebrates. *PLoS One* **7**, e49265.

**Zhao, X., Guo, F., Liu, F., Cuconati, A., Chang, J., Block, T. M. & Guo, J. T. (2014).** Interferon induction of IFITM proteins promotes infection by human coronavirus OC43. *Proceedings of the National Academy of Sciences of the United States of America* **111**, 6756-6761.

**Zhou, P., Cowled, C., Wang, L. F. & Baker, M. L. (2013).** Bat Mx1 and Oas1, but not Pkr are highly induced by bat interferon and viral infection. *Developmental and comparative immunology* **40**, 240-247.

**Zhou, P., Cowled, C., Todd, S., Crameri, G., Virtue, E. R., Marsh, G. A., Klein, R., Shi, Z., Wang, L. F. & other authors (2011).** Type III IFNs in pteropid bats: differential expression patterns provide evidence for distinct roles in antiviral immunity. *J Immunol* **186**, 3138-3147.

**Zufferey, R., Nagy, D., Mandel, R. J., Naldini, L. & Trono, D. (1997).** Multiply attenuated lentiviral vector achieves efficient gene delivery in vivo. *Nature biotechnology* **15**, 871-875.

724 **Figure Legends**

725

726 **Figure 1. Multiple sequence alignments with microbat and pig IFITM3.** (**a**) Pig and
727 microbat IFITM3 nucleotide sequences were aligned with experimentally verified IFITM3
728 orthologues. The intron-exon boundary is shown (exon1: black, exon 2: blue) and intronic
729 sequences flanking the splice sites are in red lower case. * denotes identical nucleotides. (**b**)
730 Pig and microbat IFITM3 amino acid sequences were aligned with other IFITM proteins. '*'
731 indicates identical amino acid residues, ':' indicates residues with strongly similar properties,
732 '.' indicates residues with weakly similar properties. The arrow indicates the exon-exon
733 boundary. Protein domains of human IFITM3 are shown (according to (John *et al.*, 2013))
734 (intramembrane domain 1 (IM1), conserved intracellular loop (CIL) and intramembrane
735 domain 2 (IM2)). Highlighted residues are discussed within the text.

736

737 **Figure 2. Subcellular localization of IFITM3 proteins.** A549 cells stably expressing HA-
738 tagged IFITM3 proteins from human, pig or microbat (or untransduced cells) were fixed,
739 permeabilised and stained for HA, CD63 (**b**) or LAMP1 (**c**). In (**a**) cells were incubated with
740 Alexa 546-conjugated transferrin before fixation and staining with FITC-conjugated anti-HA.
741 Nuclei were stained with DAPI and coverslips examined by confocal microscopy. Images
742 show representative staining patterns. Scale bar measures 10 um. Arrows in (**b**) identify
743 'ring-like' staining of microbat IFITM3-HA and CD63.

744

745 **Figure 3. Endocytic uptake of IFITM3 proteins**. Live A549 cells expressing HA-tagged
746 IFITM3 from human, pig or microbat (or untransduced cells) were incubated either on ice (**a**)
747 or at 37$^{o}$C (**b)** with FITC-conjuated anti-HA and Alexa 546-conjugated transferrin. After cell
748 fixation, nuclei were stained with DAPI, and coverslips examined by confocal microscopy.
749 Scale bar measures 10 um.

750

751 **Figure 4. Microbat and pig IFITM3 inhibit influenza HA-mediated cell**

**entry**. A549 cells stably expressing IFITM3 from human, pig (**a**) or microbat (**b**) (or untransduced cells) were infected with pseudotyped viruses which express different influenza HA glycoproteins. 48h post-infection, luciferase reporter activity was measured and normalized to untransduced cells (relative infectivity of 1 corresponds to 3,000-5,000 relative light units according to pseudotype used). Mean+ SD is shown (n=3) and data is representative of 3 independent experiments.

**Figure 5. Microbat and pig IFITM3 inhibit influenza virus replication**. A549 cells stably expressing human, pig or microbat IFITM3 were infected with influenza A virus. In (**b**)-**(d)** pig IFITM3 clone 1 and microbat IFITM3 clone 2 were used. (**a**) 7h post-infection with influenza A/WSN/33 NP expression was analysed by flow cytometry. (**b**) 16h after infection with influenza A/WSN/33 or A/swine/453/06 or mock-infection (-V) cells were lysed and Western blotting performed to detect influenza NP, actin and HA-tagged IFITM3 or GFP. Molecular weight (MW) of protein size markers is indicated. Virus yields following infection with influenza A/WSN/33 at m.o.i. 3 (**c**) or m.o.i. 0.01 (**d**) were measured using plaque assays. Mean+ SD is shown (n=3). *: $p<0.05$, **: $p<0.01$ and ****:$p<0.0001$ relative to GFP-expressing cells (Student's *t* test).

**Figure 6. Microbat and pig IFITM3 inhibit cell entry mediated by lyssavirus G proteins**. A549 cells stably expressing either GFP, human IFITM3, pig IFITM3 (clone 1) or microbat IFITM3 (clone 2) were infected with pseudotyped viruses which express the envelope glycoprotein from MOKV (Mokola virus), WCBV (West Caucasian Bat Virus), LBV (Lagos Bat Virus) or ERA (Evelyn Rokitniki Abelseth rabies strain). 48h post-infection, luciferase reporter activity was measured and normalized to GFP-expressing cells (relative infectivity of 1 corresponds to 25,000-80,000 relative light units according to pseudotype used). Mean+ SD is shown (n=3) and data is representative of 3 independent experiments.

**Figure 7. Microbat and pig IFITM3 are polyI:C responsive**. Pig NPTr (**a**) and microbat (**b**) cells were either mock-treated or stimulated by addition of polyI:C to cell media (50ug/ml) or transfection of polyI:C (33ug/ml) using Lipofectamine 2000 (microbat cells only). 7h later qRT-PCR was used to quantitate IFITM3 and the reference gene GAPDH. Fold change in IFITM3 mRNA is expressed relative to mock-treated cells. Mean+ SD shown for biological triplicates assayed in duplicate.

**Figure 8. siRNA knockdown of IFITM3 in pig and microbat cells enhances influenza virus replication**. Pig NPTr or microbat cells were transfected with siRNA targeting IFITM3 or control siRNA prior to quantitation of IFITM3 by qRT-PCR (**a** & **e**) or infection with influenza A/WSN/33. Virus yields were measured by plaque assay (**b**, **f**) or NP expression was measured using flow cytometry (**c, d, g**). NPTr cells were either stimulated with polyI:C for 2h before infection (m.o.i. 0.01) and analysed 36 h post-infection (**b** & **c**) or otherwise cells were infected in the absence of polyI:C. Mean+ SD shown for biological triplicates assayed in duplicate and data is representative of 2 independent experiments. *: $p<0.05$ and **: $p<0.01$ (Student's *t* test).

Figure 1

Click here to download Figure: Figure1.pdf

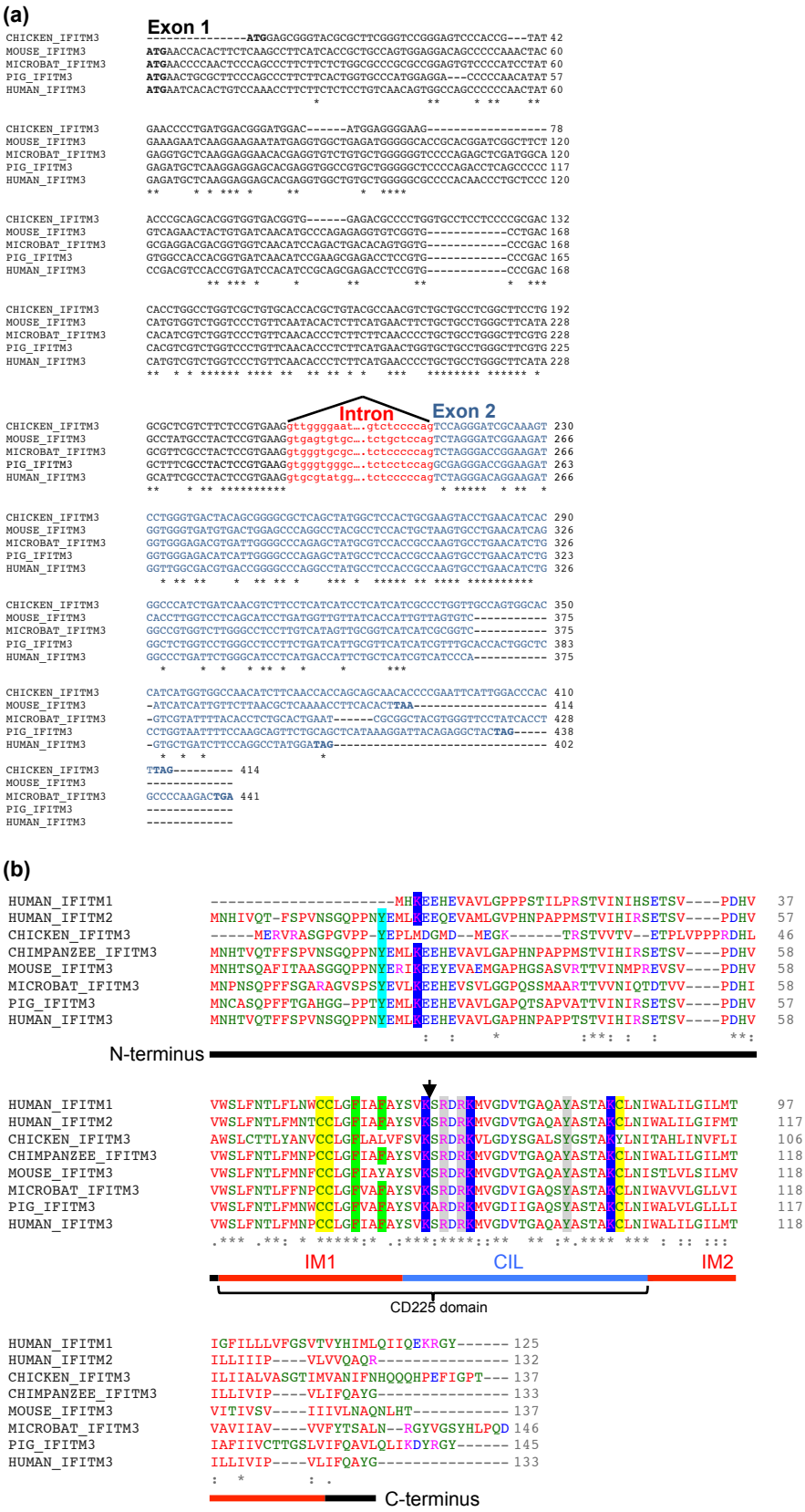

Figure2
Click here to download high resolution image

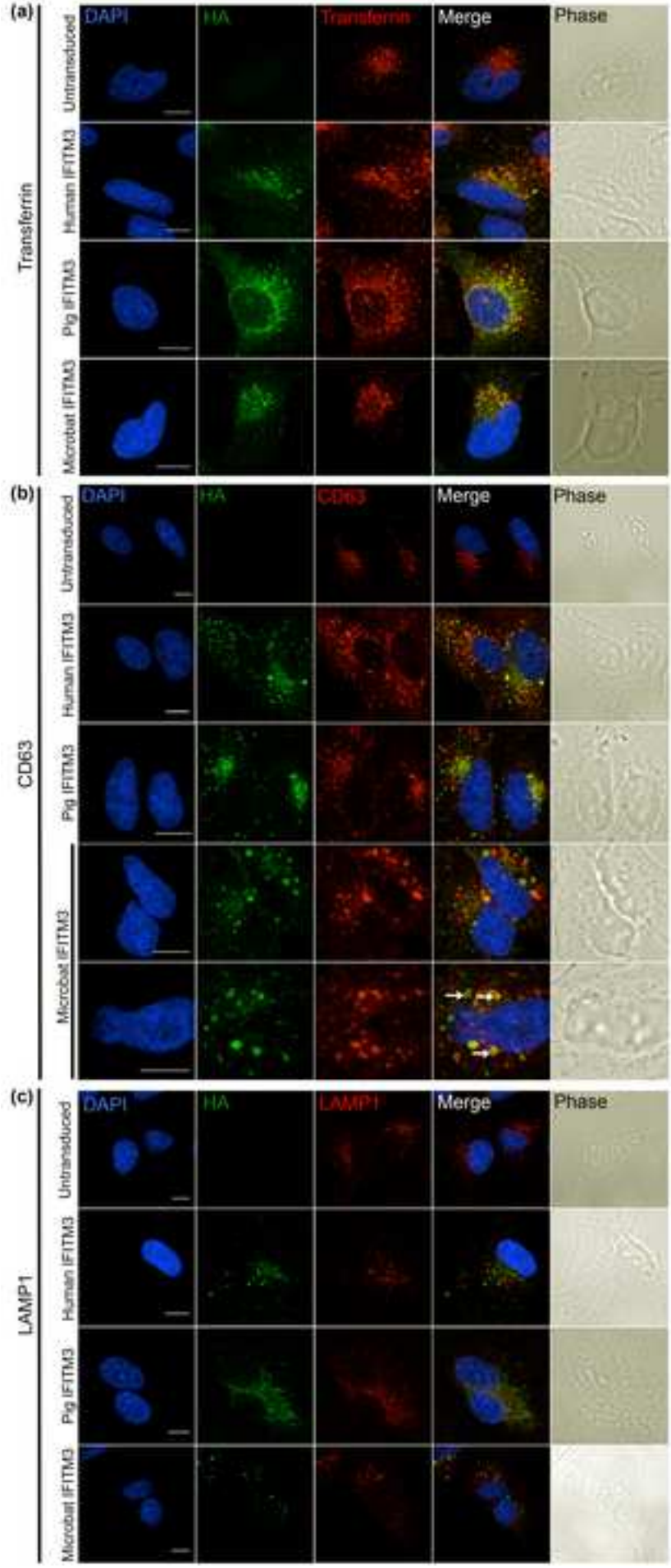

Figure3
Click here to download high resolution image

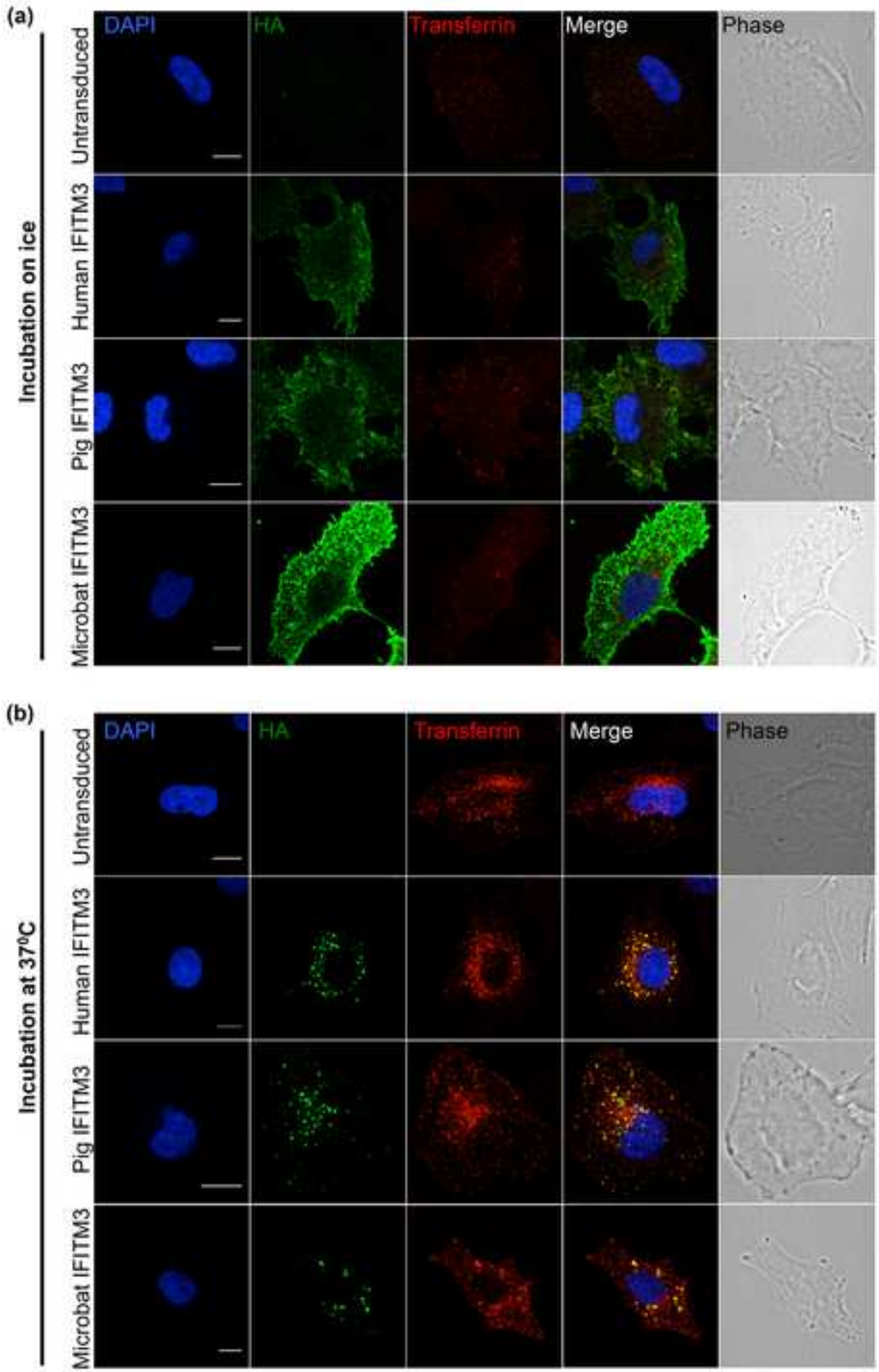

Figure4
Click here to download Figure: Figure4.pdf

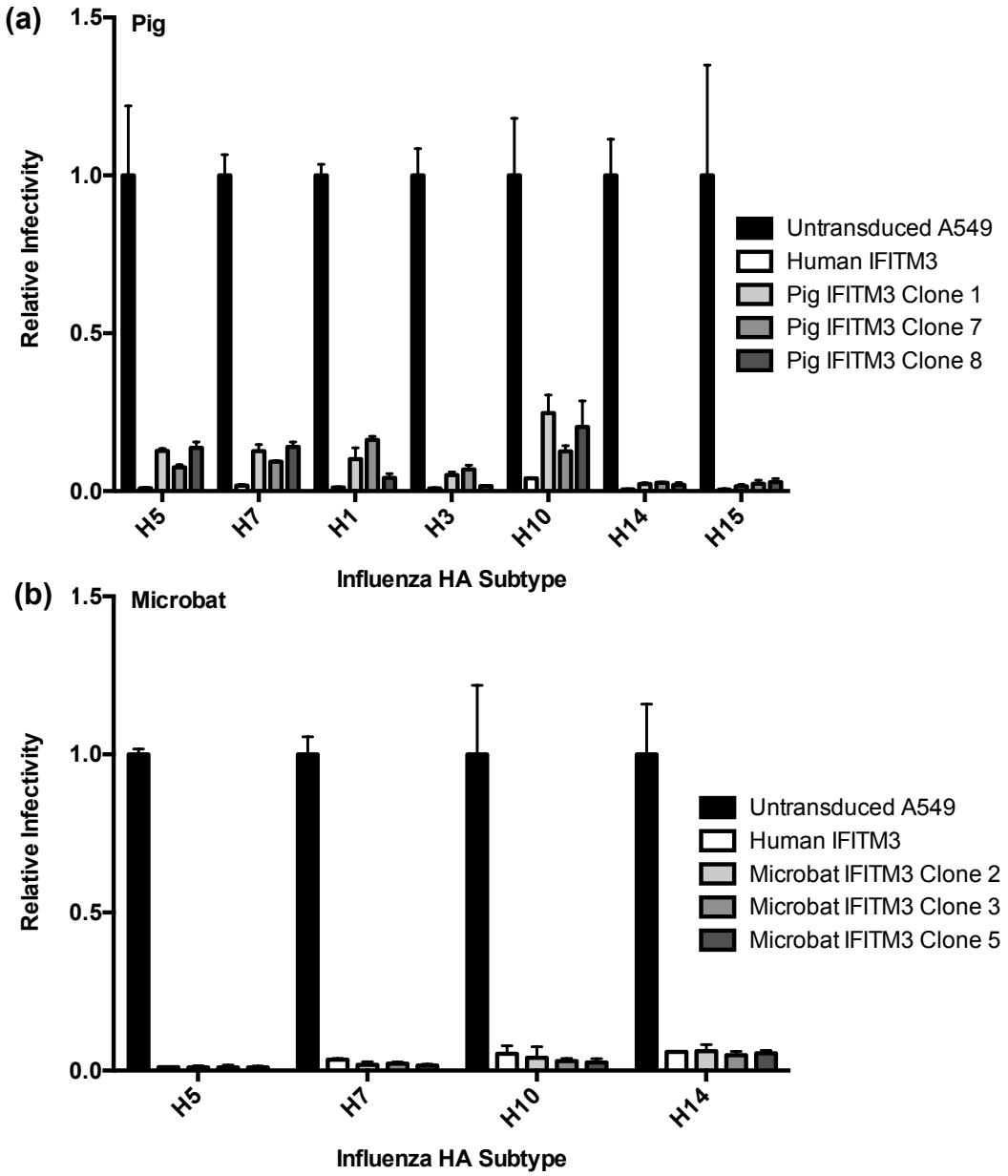

Figure5
Click here to download Figure: FIGURE5.pdf

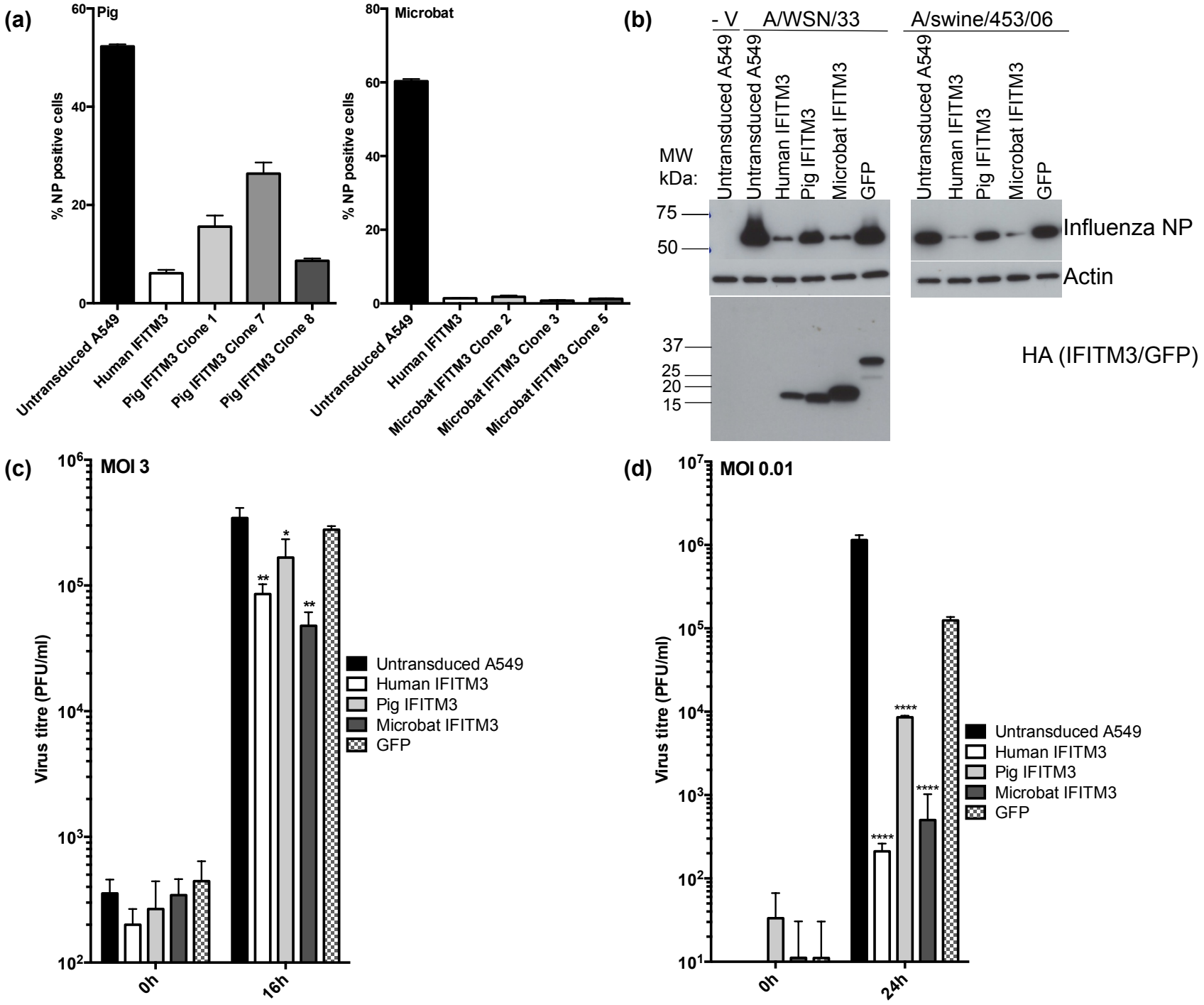

Figure6
Click here to download Figure: Figure6.pdf

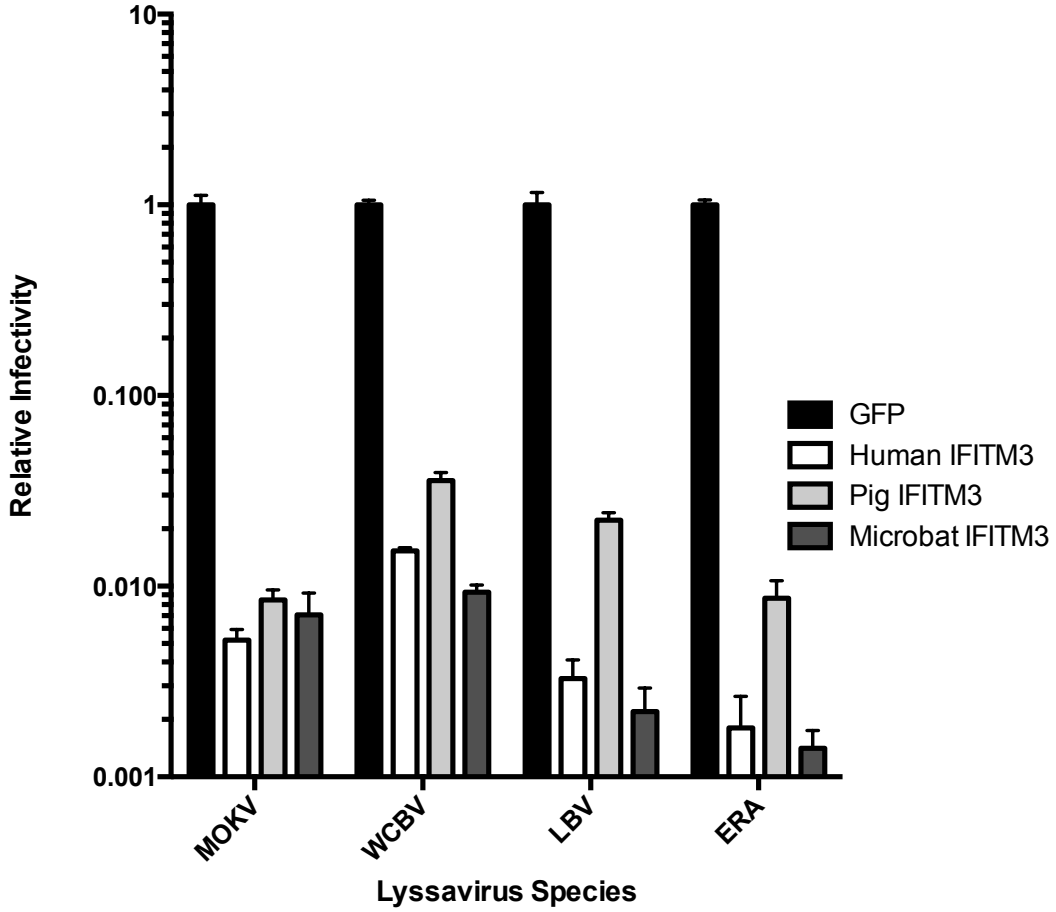

Figure7
Click here to download Figure: FIGURE7.pdf

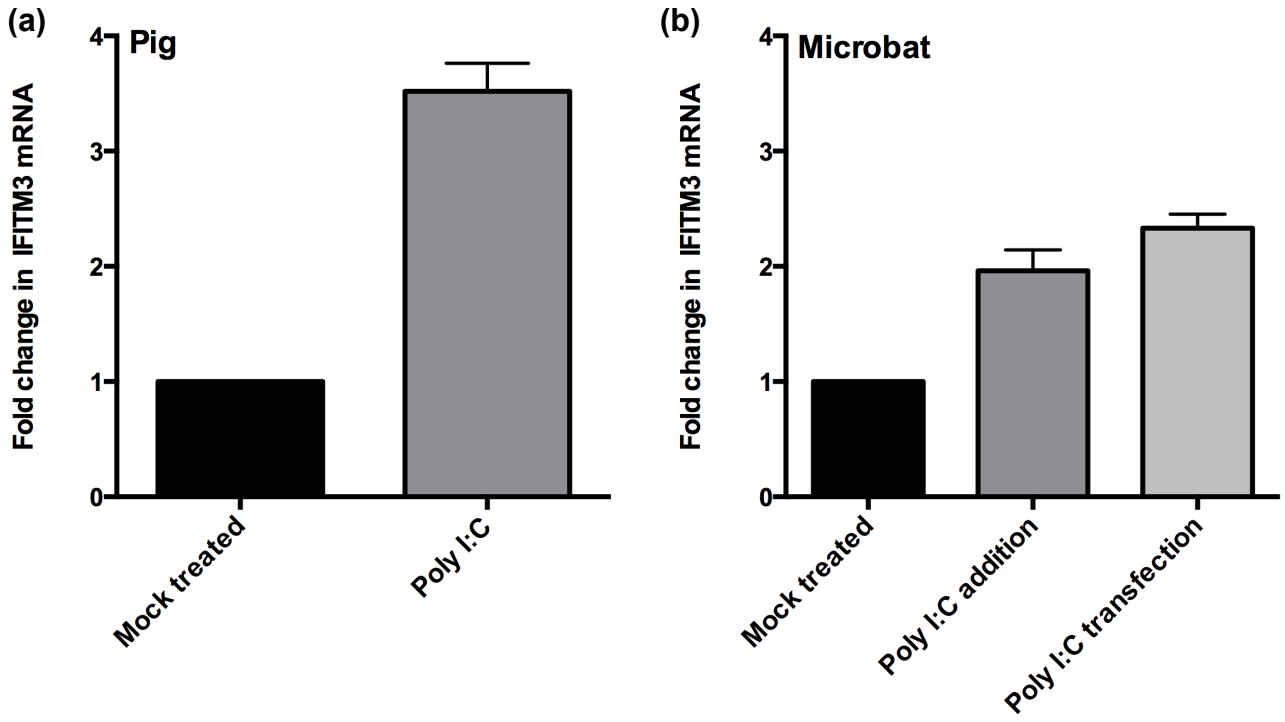

Figure8
Click here to download Figure: FIGURE8.pdf

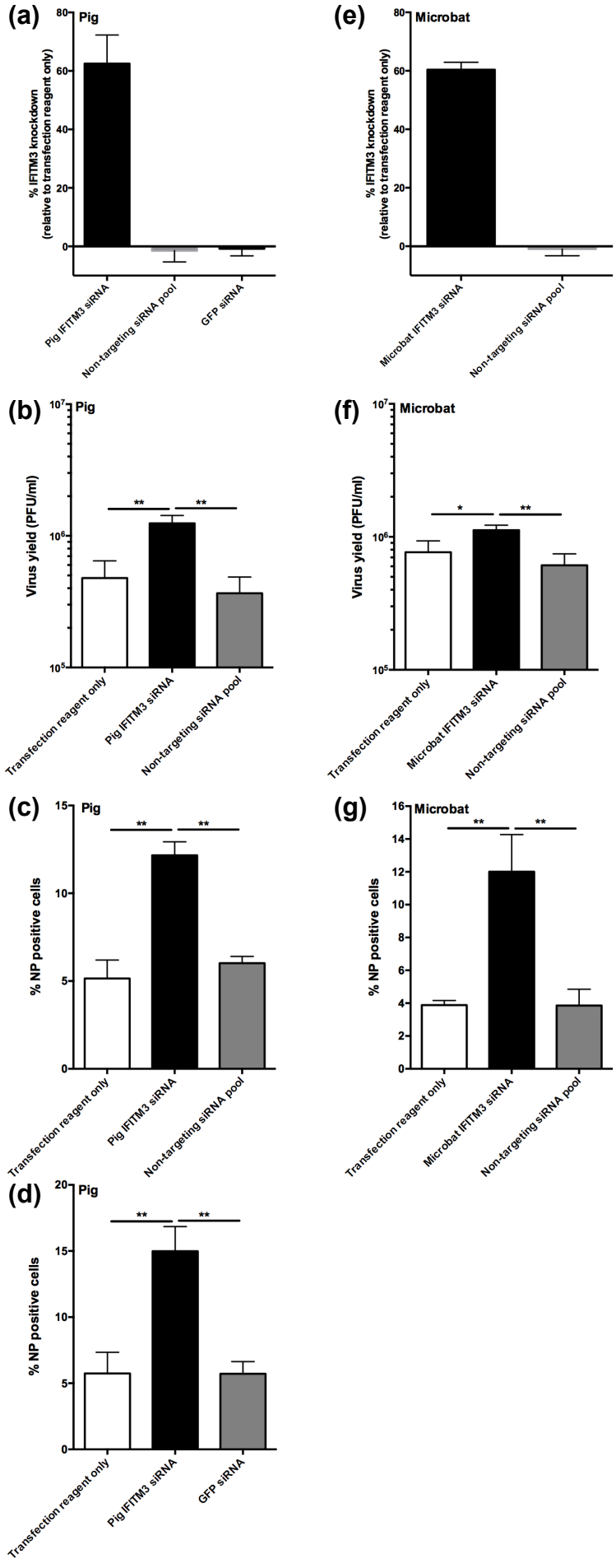

Supplementary Material Files

Click here to download Supplementary Material Files: Supplementary data.pdf